Biosensors and Bioelectronics 205 (2022) 114086

Contents lists available at ScienceDirect

Biosensors and Bioelectronics

journal homepage: www.elsevier.com/locate/bios

A GMR-based assay for quantification of the human response to influenza

Neeraja Ravi [a,*], Sarah E. Chang [b,c], Luis M. Franco [d], Sandesh C.S. Nagamani [e], Purvesh Khatri [c,f], Paul J. Utz [b,c], Shan X. Wang [g,h]

[a] Department of Bioengineering, Stanford University, Stanford, CA, 93405, USA
[b] Institute for Immunity, Transplantation and Infection, Stanford University School of Medicine, Stanford, CA, USA
[c] Division of Immunology and Rheumatology, Department of Medicine, Stanford University School of Medicine, Stanford, CA, USA
[d] Functional Immunogenomics Unit, Systemic Autoimmunity Branch, National Institute of Arthritis and Musculoskeletal and Skin Diseases, National Institutes of Health, Bethesda, MD, USA
[e] Department of Molecular and Human Genetics, Baylor College of Medicine, Houston, TX, USA
[f] Division of Biomedical Informatics, Department of Medicine, Stanford University, Stanford, CA, USA
[g] Department of Materials Science and Engineering, Stanford University, Stanford, CA, USA
[h] Department of Electrical Engineering, Stanford University, Stanford, CA, USA

ARTICLE INFO

Keywords:
GMR sensors
Influenza
Host response
Gene expression
Point-of-care diagnostics

ABSTRACT

Detecting and quantifying the host transcriptional response to influenza virus infection can serve as a real-time diagnostic tool for clinical management. We have employed the multiplexing capabilities of GMR sensors to develop a novel assay based on the influenza metasignature (IMS), which can classify influenza infection based on transcript levels. We show that the assay can reliably detect ten IMS transcripts and distinguish subjects with naturally acquired influenza infection from those with other symptomatic viral infections (AUC 0.93, 95% CI: 0.82–1.00). Separately, we validated that the gene *IFI27*, not included in the IMS panel, has very high single-biomarker accuracy (AUC 0.95, 95% CI: 0.90–0.99) in stratifying patients with influenza. We demonstrate that a portable GMR biosensor can be used as a tool to diagnose influenza infection by measuring the host response, simultaneously highlighting the power of immune system metrics and advancing the field of gene expression-based diagnostics.

1. Introduction

Respiratory viral infections are a significant burden, causing 35.6 million illnesses, 710,000 hospitalizations, and 56,000 deaths annually in the United States (CDC, 2021b), and up to 4 million deaths each year worldwide (Forum of International Respiratory Societies, 2017). Globally, influenza causes 1 billion cases, 3–5 million severe illnesses, and up to 500,000 deaths annually (WHO, 2018). Seasonal and pandemic strains of influenza viruses remain among the most common and deadly respiratory viral pathogens.

Current methods for influenza testing rely on the detection of influenza viral antigens or RNA. Rapid influenza diagnostic tests (RIDTs) are antigen-based tests that can be done at the point-of-care (POC), typically within 30 min. However, these tests are qualitative and provide only a dichotomous result of either the presence or absence of the influenza virus without quantifying viral load; the sensitivity of such tests is estimated to be between 50 and 70% (CDC, 2016). The gold standard for influenza testing is reverse transcription polymerase chain reaction (RT-PCR), in which amplification of influenza viral RNA is performed and quantified. However, the primers for RT-PCR testing are designed to detect specific viral sequences and the diagnostic efficacy can be reduced when a new strain emerges in the population.

While detection of viral RNA is important for disease diagnosis, exploring differences in host gene expression during the time course of infection could provide useful clinical information. For example, a rapid and quantitative snapshot of the body's active immune response could be tested in clinical studies as a tool to inform decisions regarding dose and duration of antiviral medications. A multi-cohort analysis of publicly available transcriptional data, leveraging the heterogeneity present in five influenza gene expression data sets with 292 samples in total, identified an 11-gene host response signature, the Influenza Meta Signature (IMS), that could distinguish individuals infected with

* Corresponding author. 476 Lomita Mall, Stanford, CA, 94305, USA.
E-mail addresses: neravi@stanford.edu (N. Ravi), sarahechang14@gmail.com (S.E. Chang), luis.franco@nih.gov (L.M. Franco), nagamani@bcm.edu (S.C.S. Nagamani), pkhatri@stanford.edu (P. Khatri), pjutz@stanford.edu (P.J. Utz), sxwang@stanford.edu (S.X. Wang).

https://doi.org/10.1016/j.bios.2022.114086
Received 14 October 2021; Received in revised form 12 January 2022; Accepted 7 February 2022
Available online 17 February 2022

influenza from those with bacterial or other respiratory viral infections (Andres-Terre et al., 2015). The level of expression of these genes is summarized by the IMS Score (the geometric mean of the normalized expression of the eleven upregulated genes). Rapid quantification of IMS transcripts in blood with a sensitive tool could therefore serve as a diagnostic of influenza infection, which could then be assessed further for clinical utility.

While RT-PCR is the gold standard in gene expression analysis, it requires instrumentation that is unlikely to be available in settings other than a diagnostic laboratory (CDC, 2021a), which increases turnaround time for clinical applications. The same is true of gene expression microarrays, which are known to profile transcripts more easily at a larger scale, but have a lower dynamic range, as they are constrained by limitations such as fluorescent background signal and signal saturation (Zhao et al., 2014). With improved dynamic range, sensitivity, and specificity, next-generation sequencing (NGS) has become prevalent for high-throughput gene expression analysis; however, the high cost, complex equipment, and turnaround time render it impractical for rapid and targeted gene expression analysis of a limited number of genes (Arts et al., 2017).

To address these issues, we developed portable giant magnetoresistive (GMR) biosensors as a platform for targeted gene expression analysis. GMR biosensors have been shown to detect proteins (Park et al., 2016; Krishna et al., 2016), antibodies (Lee et al., 2016), enzymes (Adem et al., 2020), as well as DNA (Wang et al., 2014; Rizzi et al., 2017; Nesvet et al., 2021) with high sensitivity and specificity. In fact, previous research has shown advances in GMR sensors used for DNA biomarker detection, such as genotyping of the human hepatitis B virus (HBV) (Zhi, X. et al., 2012), with an impressive limit of detection of around 10 copies/mL of target HBV DNA molecules (Zhi, X. et al., 2014).

GMR sensors function through localized proximity magnetic sensing: magnetic nanoparticles are used as DNA tags to generate a magnetic field that is detected by the GMR biosensor, so that binding of DNA to the sensor surface can be detected in real time. Compared to traditional optical detection, advantages of magnetic sensing include a lower limit of detection, higher dynamic range, temperature insensitivity, and lower background noise (Xu et al., 2008; Rizzi et al., 2017). Since the GMR chip has 80 different sensors, the device is strong in multiplexing compared to other platforms (Ravi et al., 2018). Moreover, we have previously developed a rapid GMR platform that can interface with a smartphone, interpret data in real time and transmit results to central databases, enabling POC decision-making (Choi et al., 2016). It is generally easier to accommodate a large number of sensors in a single GMR biochip reported here than in a single giant magnetoimpedance (GMI) biochip (Gao et al., 2016).

Here, we present an assay for multiplexed transcript detection on a GMR platform that can reliably quantify the IMS score. With this assay, we show that we can accurately detect influenza virus infection and monitor influenza progression after symptom onset, providing valuable clinical information that can aid in disease management.

2. Materials and methods

2.1. In vitro treatment, RNA extraction and reverse transcription from peripheral blood mononuclear cells (PBMCs)

PBMCs from twelve healthy donors (IRB-30494, Autoimmunity Center of Excellence at Stanford) were isolated and seeded into 10 cm dishes at around 50–60% confluency, with three plates for each donor. For each donor, one plate was treated with 2000 U/mL interferon alpha (IFN) (PBL Assay Science) overnight, one was treated with 100 ng/mL lipopolysaccharide (LPS) (Sigma-Aldrich) overnight, and one was left as an untreated control. Messenger RNA (mRNA) was extracted from each culture using the Qiagen RNeasy Mini Kit (QIAGEN) according to the manufacturer's protocol. Complementary DNA (cDNA) was synthesized using the Invitrogen Superscript III First Strand Synthesis System according to the manufacturer's protocol.

2.2. Cohort of human subjects with infection

Banked whole blood RNA samples were obtained from a study (DMID #09–0062) of healthy volunteers aged between 18 and 49. Participants were serially sampled before and during infection with a naturally occurring H1N1 influenza virus or other respiratory viruses (Zhai et al., 2015). Importantly, the healthy volunteers had not been vaccinated in the three years preceding enrollment in the study and did not receive influenza vaccination during the study. Recruitment was performed during two consecutive influenza seasons: September 2009–April 2010, and September 2010–April 2011. Peripheral whole blood samples were collected in PAXgene RNA stabilization tubes (QIAGEN) and stored at -80 °C. RNA purification was performed with the PAXgene Blood RNA system (QIAGEN). Samples from each participant were collected at baseline (early in the influenza season), when the participant was healthy. Participants who exhibited any respiratory symptoms during the season were sampled again on day 0 (day of symptom onset), day 2, day 4, day 6, and day 21. The purified RNA samples were aliquotted and stored at -80 °C, and deidentified samples from subjects that had given consent to have their samples further analyzed were transferred from Baylor College of Medicine, Houston, TX to Stanford University, Stanford, CA in August 2020. The protocol was approved by the institutional review boards of all participating institutions. Additionally, nasal wash samples on day 0 and day 2 were tested with RT-PCR for respiratory viruses including influenza A, pH1N1 influenza, influenza B, picornavirus/rhinovirus, respiratory syncytial virus, human metapneumovirus, parainfluenza viruses, coronaviruses, and adenoviruses (Zhai et al., 2015).

For the GMR data analysis at Stanford University, we selected samples from participants that were RT-PCR positive for influenza A or B viruses, human rhinovirus (HRV), and participants with flu-like symptoms in whom no virus was identified. In the process of selection, we remained blinded to the status of each participant, but chose these three classifications as they had the most samples available for a reasonable statistical analysis. From these subjects, a final cohort of 68 subjects (40 female, 28 male) was chosen that had both baseline and day 0 samples available. Four subjects were also chosen that had follow-up samples available from day 2, day 4, day 6, and day 21 post-infection. The concentration of the RNA samples for all subjects was quantified using Qubit (ThermoFisher Scientific), and the RNA was reverse transcribed to cDNA using SuperScript III First-Strand Synthesis System (ThermoFisher Scientific). Briefly, 200 ng of input mRNA was reverse-transcribed with an oligo$(dT)_{20}$ primer, using SuperScript III reverse transcriptase (RT) in a 20 μL reaction. The cDNA was stored at -20 °C prior to PCR amplification.

2.3. RT-PCR amplification

Prior to GMR detection, cDNA was RT-PCR amplified using a BioRad Thermal Cycler and primers specific to IMS genes. All primer sequences were designed with Universal ProbeLibrary System Assay Design Center (Roche), and the sequences were obtained from Integrated DNA Technologies (Table S1). The primers had a stock concentration of 100 μM and were diluted to 80 μM prior to use. SsoAdvanced Universal SYBR Green Supermix (Bio-Rad) was used for fluorescence detection, and a master mix was created with 1:10 dilution of Supermix to primers. The total volume of each qPCR reaction was 20 μL, with 2 μL of PBMC cDNA, 10 μL of master mix, and the remaining 8 μL with primers for the genes of interest and DNA suspension buffer (Teknova). For the stimulated PBMC cDNA from **Section 2.1**, primers specific to the IMS genes *HERC5*, *HERC6*, *PARP12*, *LGALS3BP*, *ZBP1*, *IFI6*, *IFIH1*, *CD38*, and *LY6E* were used (Table S1). PCR amplification was initiated with polymerase activation and DNA denaturation at 95 °C for 30 s, followed by 27 cycles with denaturation at 95 °C for 10 s, and annealing and extension at 59 °C

for 30 s. For the subject cDNA from **Section 2.2**, primers specific to the IMS genes *HERC5*, *HERC6*, *PARP12*, *LGALS3BP*, *ZBP1*, *IFI6*, *IFIH1*, *LY6E*, and *RTP4* were used, along with the *IFI27* gene (Table S1). PCR amplification was initiated with polymerase activation and DNA denaturation at 95 °C for 30 s, followed by 25 cycles with denaturation at 95 °C for 10 s, and annealing and extension at 59 °C for 30 s. A no-template control was also amplified to assess contamination levels and primer specificity.

2.4. RT-PCR fold change calculations with stimulated PBMC cDNA

Prior to GMR detection, RT-PCR was used to determine if each IMS gene was upregulated in IFN-treated healthy PBMCs compared to an untreated control. For these reactions, each IMS gene was amplified individually, and expression levels were compared between the IFN-treated sample and the control. A housekeeping gene, *GAPDH*, was amplified for both conditions to calibrate the calculations. The raw Ct values of *GAPDH*, in triplicate, were averaged for each condition, and then subtracted from the Ct values for each IMS gene for each condition. Finally, the corrected values for each gene, in triplicates, were averaged. The final fold change for each IMS gene was calculated as 2^(Control-Treated Ct).

2.5. GMR sensor preparation

The GMR biosensor arrays, comprised of 8 × 10 sensors, were fabricated as described previously (Osterfeld et al., 2008). The sensors are functionalized with amino-modified DNA probes using a surface silanization, by a method described previously (Ravi et al., 2018). Briefly, the surface was activated with a 15-min treatment with 15% hydrogen peroxide (Certified ACS, Sigma-Aldrich) in distilled water, 30-min treatment with 10% (3-aminopropyl) triethoxysilane (Sigma Aldrich) in acetone, 30 min treatment with 5% glutaraldehyde (Fisher Scientific) in distilled water, and a final wash with distilled water. Each DNA probe was diluted to 20 μM in filtered 2X saline sodium citrate SSC (Invitrogen) from a stock solution of 20X SSC prior to spotting. The DNA probes (Table S1) were spotted (~1.5 nL) onto separate sensors of the GMR chip using a robotic arrayer (sciFlexarrayer, Scienion). For each chip, 7 sensors were functionalized with the probes complementary to each of the 10 IMS genes used (70 sensors total), 4 sensors were functionalized with a DNA sequence not complementary to the PCR-amplified product, as a negative control, and 4 sensors were functionalized with biotinylated DNA as a positive control. The chips were stored at room temperature until use. Prior to use, the GMR chips were inserted into cartridges defining a reaction well over the sensors. The chip surface was then washed and blocked with 1% BSA in PBS for 30 min as described previously (Osterfeld et al., 2008) to prevent non-specific binding.

2.6. Addition of PCR product to GMR sensors

Double-stranded PCR products with amplified IMS genes prepared at the end of **Section 2.3** were added to the GMR sensors prepared at the end of **Section 2.5**. 20 μL of the PCR product was added to 130 μL hybridization buffer (400 mM NaCl in Tris EDTA). The PCR product denatured through a modified heat and shock-cooling denaturation approach as described previously (Rizzi et al., 2017). Briefly, the samples were denatured for 10 min at 95 °C and shock-cooled for 5 min in ice to slow down re-hybridization. The denatured samples were inserted onto the GMR chip, and allowed to hybridize to the DNA probes on the chip for 1 h at 37 °C. The chips were then washed six times with washing buffer (10 mM NaCl in Tris EDTA) to remove unbound DNA, leaving around 50 μL wash buffer on the sensor surface. The GMR cartridges were inserted into the MagArray reader stations. After measuring 2 min of baseline signal and allowing calibration of the sensor system, 50 μL of streptavidin magnetic nanoparticles (MNPs) (Miltenyi Biotec) were added in the sample well and the binding signal was measured at 15 min when the GMR signal reached a plateau, indicating binding saturation. DNA hybridization causes magnetic nanoparticles to bind to the sensor surface, leading to a change in the measured magnetoresistive (MR) ratio of the sensor. The signal is measured in terms of $\Delta MR = MR - MR_0$. All samples for each condition were run in duplicate.

2.7. IMS gene expression measurements and analysis: infection cohort

The endpoint GMR binding signals in parts per million (ppm) across all subjects were extracted, and the signal from the negative control was subtracted to control for background noise. For each gene, there were 7 sensors per chip, and 2 chips per time point; the 14 binding signals were averaged to get a mean expression for that gene (individual outlier sensors that were greater/lower than two standard deviations from the mean were disregarded in the average calculation).

For the stimulated PBMC experiments, average expression measurements were rescaled to a value between 0 and 100, and the fold change for each gene was calculated by dividing the average expression in each condition (either LPS or IFN) by the average expression in the control condition. A paired *t*-test was conducted to examine statistical significance between the LPS and IFN groups for each gene (a two-tailed p-value < 0.05 was significant). For each subject, the fold change across all individual IMS genes was averaged to find the total IMS fold change score for each subject. Fold change analysis was done in R (R Core Team, 2019); statistical tests and graph generation were done in GraphPad Prism (Version 8.4.1).

For the infection cohort experiments, the average expression measurements for each gene were $\log_2$ transformed, and the geometric mean of the $\log_2$-transformed genes was calculated for each subject at baseline and on day 0 (day of symptom onset), to obtain the IMS score (Andres-Terre et al., 2015). The $\log_2$ transformation and geometric mean calculations were performed in R (R Core Team, 2019). The day 0 classifications of the 68 subjects were then unblinded, and a Mann-Whitney test was performed to determine if the day 0 IMS score was significantly different in subjects with influenza virus infection, HRV infection, or individuals with respiratory symptoms who tested negative for the viruses interrogated by the RT-PCR virology panel. A Mann-Whitney test was also performed to determine if the day 0 individual log2-transformed gene expression was significantly different in subjects with influenza virus infection, HRV infection, or with a "negative" classification. For both tests, a two-tailed p-value < 0.05 was significant.

A Wilcoxon matched-pairs signed rank test was performed for individuals with confirmed influenza to determine if the baseline IMS score was significantly different from the day 0 IMS score. The difference in baseline and day 0 scores was calculated for each influenza subject and a Mann-Whitney test was performed to determine if the IMS scores were significant between timepoints. A two-tailed p-value < 0.05 was considered significant. Statistical tests and graph generation were conducted in GraphPad Prism (Version 8.4.1).

Additionally, two influenza-infected subjects, one HRV-infected individual, and one "negative" subject that had RNA samples available from multiple time points after symptom onset were selected for follow-up analysis. The IMS score for these subjects was calculated and plotted over the course of baseline to day 21 for the influenza-infected subjects, and baseline to day 6 for the non-influenza infected subjects, to examine gene expression kinetics after infection.

2.8. Logistic regression models and ROC curve analysis

Using all data (n = 68), logistic regression models were developed to determine if the expression level of the IMS biomarkers could diagnose influenza infection status. Influenza-infected subjects were treated as cases, and HRV-infected and negative subjects were grouped together as non-influenza, or control. A univariate logistic regression model using IMS scores at the day of symptom onset was developed and evaluated.

The data was then split into training (42 subjects) and test (26 subjects) sets using the R caret package, and a multivariate logistic regression model using all individual IMS genes was developed on the training set and evaluated on the separate, withheld test set, using the glm() function in R's built-in stats package. The pROC package in R was used to develop Receiver-Operating Characteristic (ROC) curves on the test set and extract the AUC of each model; GraphPad prism was utilized to plot the ROC curves. The diagnostic power of *IFI27* was additionally examined through a univariate logistic regression model (n = 68).

A regression model was developed with the L1 penalty for feature selection to assess which individual IMS genes in conjunction with *IFI27* were most beneficial for influenza classification. L1 regularization, or LASSO regression, adds a penalty equal to the sum of the absolute value of the coefficients, thereby shrinking certain parameters to zero to prevent overfitting on an unseen test dataset. The glmnet package in R was utilized for L1 regression. After the model was developed, the regression coefficients were summarized, and the coefficients with weights greater than zero were selected as important features. The test set AUC was then determined using these four individual gene expression values.

3. Results

We used GMR sensors for multiplexed gene expression quantification by magnetically detecting biotinylated PCR products after reverse transcription from sample mRNA and performing targeted amplification of the IMS genes (Fig. 1). The GMR chips were spotted according to the spotting pattern shown in Fig. S1. There was no cross reactivity between individual amplified IMS genes and their corresponding GMR probes; each gene only bound to its respective probe (Fig. S2).

3.1. IMS genes are upregulated after in vitro IFN stimulation of PBMCs

The interferon (IFN) response is one of the first barriers of defense against influenza viruses. Specifically, type I IFNs, such as IFN-alpha, are secreted after influenza infection and are critical in hindering viral replication and proliferation (Killip, M. et al., 2015). Before measuring IMS expression through GMR, we used RT-PCR to determine if IMS genes were upregulated in IFN-treated PBMCs compared to controls. Each IMS gene was amplified individually, and its expression was compared between control and IFN-treated PMBCs. We found that all IMS genes were upregulated (fold change>1) in IFN-treated PBMCs compared to controls (Fig. S3). Fold change values ranged from 6.2 (*IFI6*) to 46.6 (*ZBP1*).

3.2. IMS gene expression measured by GMR sensors is higher after IFN than after LPS stimulation

Bacterial lipopolysaccharides (LPS), also known as an endotoxins, are present in the outer surface membrane of Gram-negative bacteria, and are implicated in the pathogenesis of sepsis (Opal, 2010). For our study, IFN-alpha was used as a virus-specific immune modulator, and LPS was used as a non-specific immune modulator.

To determine if the IMS biomarkers were indeed virus specific, IFN-

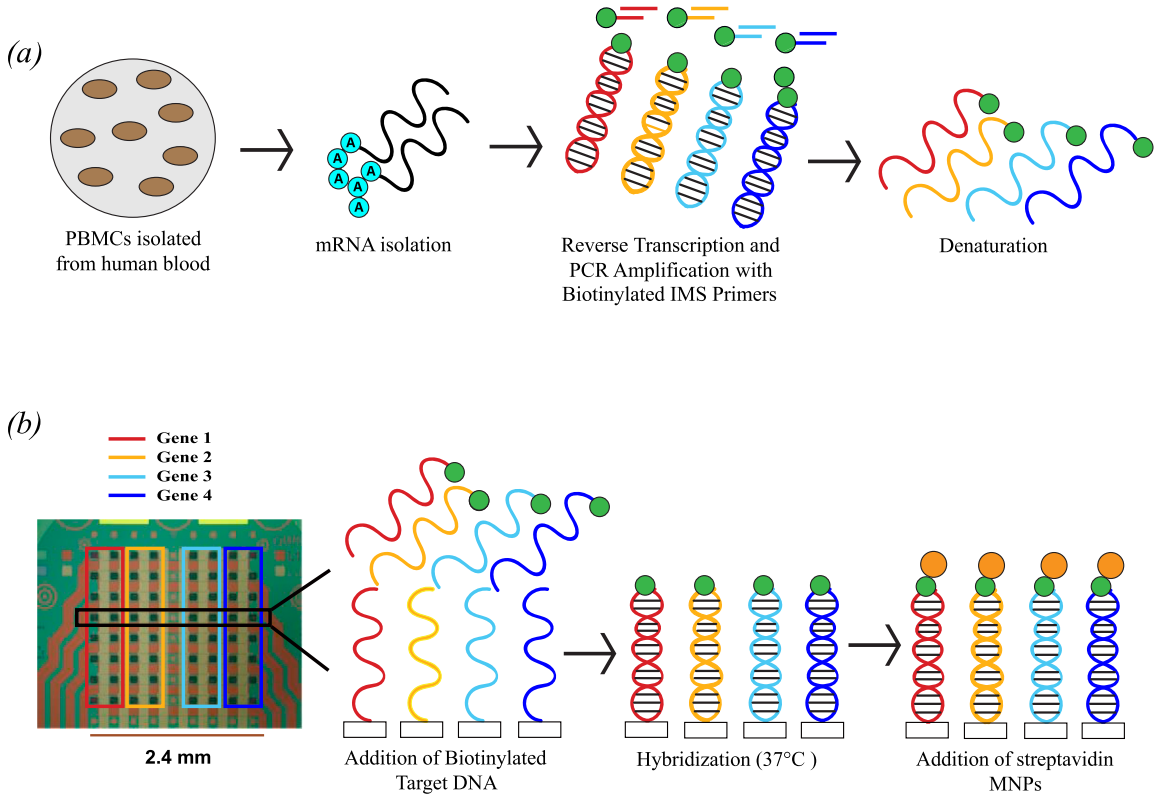

Fig. 1:. Workflow for detection of IMS genes on the GMR biosensor array. (a) PBMCs were isolated from healthy human donors. mRNA was isolated, reverse-transcribed to cDNA, and PCR-amplified with biotinylated primers for the IMS genes of interest. The PCR product was denatured at 95 °C to create biotinylated ssDNA corresponding to each of the target IMS genes. (b) Sensors on the GMR chip are spotted with ssDNA probes complementary to each of the IMS genes seen in (a), along with a negative control and a positive control, according to the simplified spotting pattern seen. The target ssDNA is added to the sensor surface and allowed to hybridize. Signal is measured after adding streptavidin MNPs. To simplify, only four of the nine IMS genes are shown; for full spotting pattern, see Fig. S1.

stimulated, LPS-stimulated, or control PBMC-derived cDNA samples were amplified with primers specific to IMS genes, and the fold change of each individual gene relative to control was calculated, along with the mean fold change across all IMS genes for each condition. The mean fold change across all IMS genes, or the IMS fold change, was significantly higher in IFN-treated PBMCs compared to LPS-treated PBMCs ($p < 0.0001$; Fig. 2a). Similarly, the fold change for each individual IMS gene was significantly higher in IFN-treated PBMCs compared to LPS-treated PBMCs for all donors (Fig. 2b). The strongest differentiators between IFN and LPS treatment were *IFI6*, *HERC5*, *HERC5*, and *LY6E* ($p < 0.0001$), followed by *PARP12*, *IFIH1*, *CD38*, *LGALS3BP* ($p < 0.001$), and *ZBP1* ($p < 0.01$).

3.3. IMS measured on GMR sensors distinguishes influenza from other viral respiratory infections

To determine if the IMS could distinguish influenza infection at the time of symptom onset, we measured the IMS score of subjects at day 0 using GMR sensors. Influenza-infected subjects had an overall higher IMS score compared to HRV-infected subjects or "negative" subjects ($p < 0.0001$, $n = 54$) (Fig. 3a). Here, "negative" is defined as subjects who were symptomatic but not found to have any of the 21 viruses in the RT-PCR virology panel performed on nasal wash fluid. Importantly, a statistically significant difference in the IMS score was not observed between HRV-infected subjects and negative classifications on day 0, suggesting that the IMS score is influenza-specific. To verify that the IMS score was not high before symptom onset, we measured the IMS score at the baseline timepoint, which was collected at the beginning of the influenza season, when subjects were asymptomatic. For each infection classification present in our cohort, the IMS score at baseline was lower than the IMS scores at day 0 for each subject, confirming that the increase in the IMS score was indeed attributed to the infection. The difference in IMS score between the baseline and symptom-onset (day 0) time points for influenza-infected subjects is shown in Fig. 3b.

To further investigate the difference in the IMS scores on day 0, we analyzed the $\log_2$-transformed gene expression GMR signal of each IMS gene between the classifications. Each IMS gene individually had significantly higher expression in influenza-infected subjects compared to HRV-infected subjects ($p < 0.0001$, $n = 39$) or negative subjects ($p < 0.0001$, $n = 41$) (Fig. 4). This indicates that no single gene was disproportionately driving the IMS score to be significantly different between disease classifications.

3.4. IMS measured on GMR sensors distinguishes influenza from other viral respiratory infections with high accuracy

To demonstrate the specificity and accuracy of the IMS score to distinguish influenza infection, we developed logistic regression models with different combinations of independent variables, in which influenza-infected subjects were treated as cases, and HRV or negative subjects were grouped together as non-influenza, or control. In a univariate logistic regression model using day 0 IMS score as the independent variable, using all the data ($n = 68$), the AUC was 0.87 (95% confidence interval (CI): 0.79–0.96) (Fig. 5a). The data was split into training (42 samples) and test (26 samples) sets, and a multivariate logistic regression model with the individual IMS gene expression values on day 0 was developed on the training set and evaluated on a separate, withheld test set with an AUC of 0.93 (95% CI: 0.82–1.00) (Fig. 5b), sensitivity of 0.81 (95% CI: 0.70–0.92) and specificity of 0.89 (95% CI: 0.51–1.00).

We then re-visited the genes that comprised the original IMS panel. One of the genes not included in the IMS panel originally was *IFI27*, which has been shown to distinguish influenza from other respiratory viral infections with a high single-biomarker accuracy (Tang et al., 2017). Therefore, we tested the ability of *IFI27* to distinguish influenza from non-influenza cases in this cohort. Fig. S4 shows that subjects with influenza had a significantly higher *IFI27* expression level compared to HRV ($p < 0.0001$, $n = 39$), or negative subjects ($p < 0.0001$, $n = 41$). We then developed a univariate logistic regression model ($n = 68$) using *IFI27* expression on day 0, resulting in a high single-biomarker AUC of 0.95 (95% CI: 0.90–0.99) (Fig. 5c).

The known interactions between the IMS genes are modeled through the STRING database (version 11.5) in Fig. S5a (Szklarczyk et al., 2021), which illustrates that the IMS genes are all part of the same transcriptional network. To determine if the biological connectivity of the genes results in experimental co-expression, the correlation coefficients between the IMS genes were calculated using the individual gene log GMR signal from the day of symptom onset. The significant coefficients are visualized using a color correlation plot (Fig. S5b). *IFI27* has the lowest individual correlations with the other IMS genes: while it is still highly correlated, its correlation coefficients range from 0.5 to 0.75, while many of the other coefficients range from 0.7 to 0.9. This reinforces the strength of *IFI27* as a biomarker for influenza infection: while groups of genes within the IMS are co-expressed as part of a broad antiviral response, *IFI27* appears to increase more independently, strongly, and specifically in influenza infection.

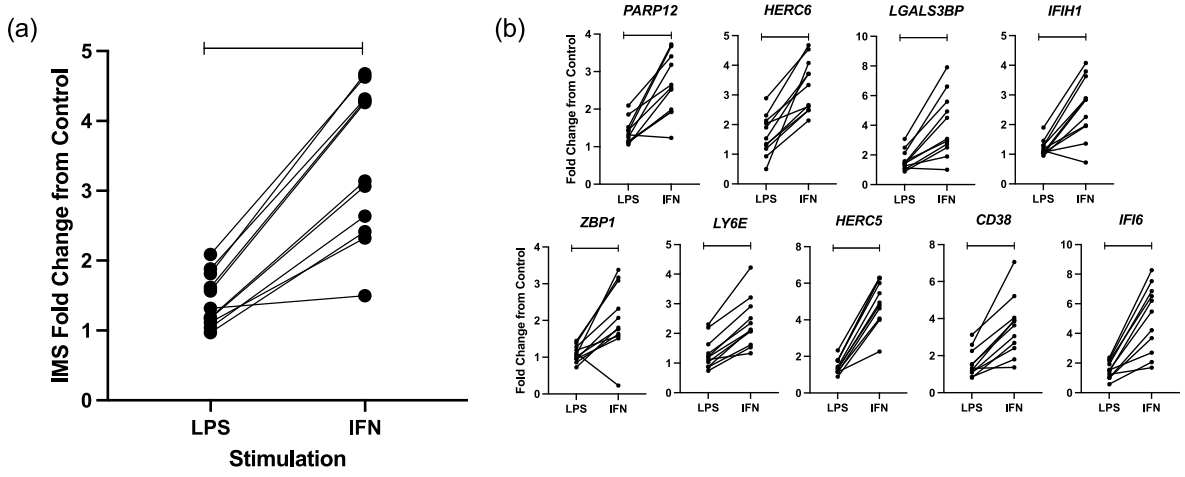

Fig. 2:. GMR levels of IMS expression examined in LPS-treated and IFN-treated healthy-donor PBMCs, each pair of dots connected by a line represents one donor. Fold change was calculated relative to untreated control. (a) For each donor, IMS expression in IFN-treated PBMCs was compared to IMS expression in LPS-treated PBMCs using a paired *t*-test ($p < 0.0001$, $n = 11$). (b) For each donor, expression levels of each individual IMS gene were compared between IFN-treated PBMCs and LPS-treated PBMCs using a paired *t*-test ($p < 0.0001$, $n = 11$).

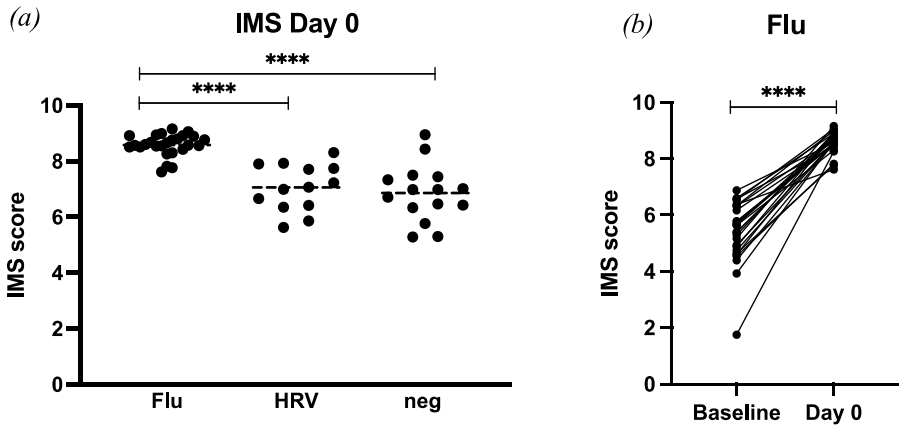

Fig. 3. (a) Subjects with flu-like symptoms were classified on the day of symptom onset (day 0) by RT-PCR on nasal wash fluid, as having influenza A or B, HRV, or negative (did not test positive for any of the viruses in the panel). Each dot represents one individual. Using a Mann-Whitney test, the IMS score on day 0 of infection was compared between influenza A or B-infected individuals, HRV-infected individuals ($p < 0.0001$, $n = 39$), or negative individuals ($p < 0.0001$, $n = 41$). (b) For influenza-infected individuals, the IMS score was compared between the baseline and day 0 timepoints using a Wilcoxon matched-pairs signed rank test ($p < 0.0001$, $n = 26$).

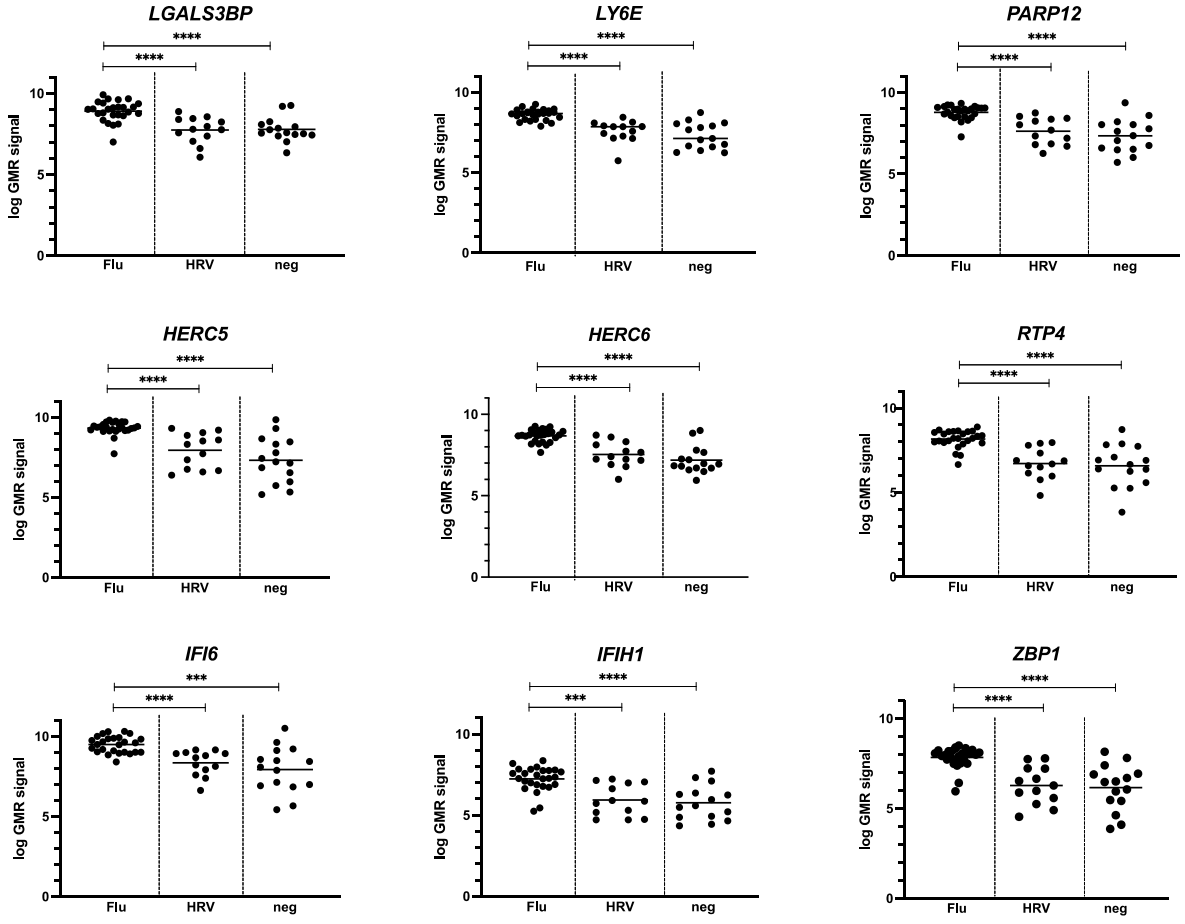

Fig. 4. Subjects with flu-like symptoms were classified on the day of symptom onset (day 0) by RT-PCR on nasal wash fluid, as having influenza A or B, HRV, or negative (did not test positive for any of the viruses in the panel). Each dot represents one individual. Expression levels of each individual IMS gene on day 0 of infection was compared between influenza A or B-infected individuals, HRV-infected individuals ($p < 0.0001$, $n = 39$), or negative individuals using a Mann-Whitney test ($p < 0.0001$, $n = 41$).

The high correlation between the IMS genes also suggested that not all genes were needed for accurate classification in this cohort. Therefore, a regression model was developed with the L1 penalty for feature selection, to assess which individual IMS genes in conjunction with *IFI27* were best able to classify influenza infection. After regularization was applied for feature selection, *IFI27*, *HERC5*, *HERC6*, and *IFIH1* had coefficients greater than 0. Using the expression levels of these four genes (now referred to as the LASSO regression score) on day 0, the test set AUC was 0.93 (95% CI: 0.84–1.00) (Fig. 5d), with a sensitivity of 0.90 (95% CI: 0.73–1.00) and specificity of 0.89 (95% CI: 0.65–1.00).

3.5. *IFI27* expression is a more stable biomarker during symptomatic infection than the IMS

To investigate the kinetics of the IMS score throughout the course of infection, we analyzed follow-up time points for two influenza-infected subjects, one HRV-infected individual, and one subject with a negative classification (Fig. 6a). Here, the IMS score includes the geometric mean

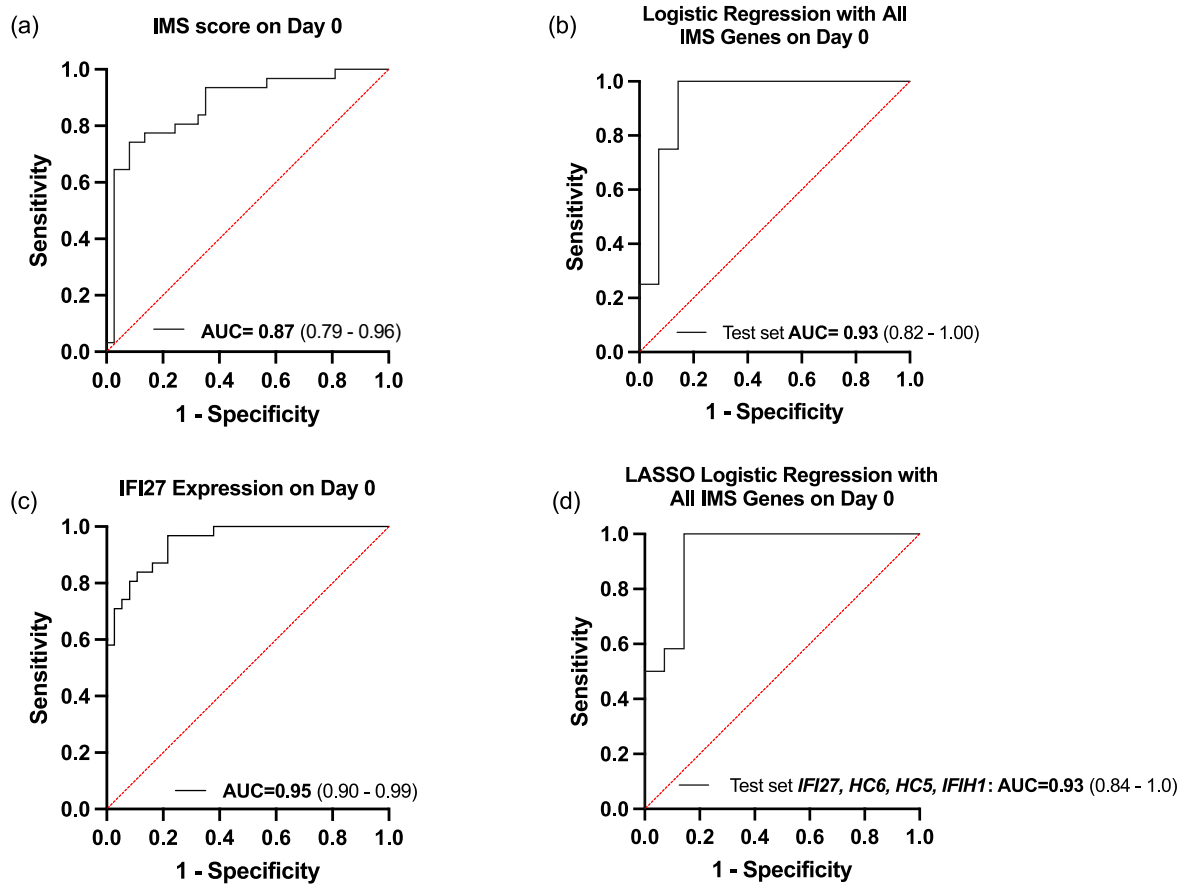

Fig. 5. Logistic regression models were applied to determine the power of the IMS genes in classifying influenza infection. (a) A univariate logistic regression model was applied using the IMS scores on day 0 (day of symptom onset); the AUC was 0.87 (95% CI: 0.79–0.96). (b) A multivariate logistic regression model was applied using the individual IMS gene scores on day 0, the test AUC was 0.93 (95% CI: 0.82–1.00). (c) The *IFI27* gene was added to the panel, and a univariate logistic regression model was developed; the AUC was 0.95 (95% CI: 0.90–0.99). (d) A multivariate LASSO logistic regression model was applied using individual IMS genes in conjunction with *IFI27*, resulting in 4 genes of greater influence. Using just the expression levels of these four genes at day 0 of infection (LASSO regression score) the test set AUC was 0.93 (95% CI: 0.84–1.00).

of the IMS genes along with *IFI27* expression. For both subjects not infected with influenza, the IMS score had minor fluctuations from baseline to day 6 post-infection. Conversely, for both influenza-infected subjects, the IMS score increased substantially from the baseline time-point to the peak score at day 0 (time of symptom onset), but after that the score decreased, returning to baseline levels on day 21. The data suggest that the ability of the IMS score to differentiate influenza from other respiratory viral diseases wanes quickly after the first day of symptoms.

Next, we examined *IFI27* expression throughout the time course of symptomatic infection. *IFI27* expression remained stable and high in influenza-infected subjects compared to the HRV or negative subjects throughout the first 6 days of symptomatic infection, returning to baseline between days 6 and 21 (Fig. 6b). Examining the time course of each of the IMS genes (Fig. 6c; Fig. 6d) in both subjects with influenza, *IFIH1* had the lowest expression levels each day, and *IFI27* had the highest expression levels until day 6. It is important to underscore that from day 0 to day 6, while *IFI27* expression levels remained stable, the expression levels of the other IMS genes progressively decreased. Our results indicate that the ability of the IMS score to differentiate influenza from other viral respiratory infections tends to decrease rapidly after the first day of symptoms, whereas *IFI27* expression remains elevated for at least six days after symptom onset.

4. Discussion

Our findings demonstrate that the portable GMR platform can be effectively applied to the quantitative, multiplexed measurement of transcript abundance. Ten transcripts, along with a negative and positive control, were simultaneously quantified. Previous studies have shown that PCR amplification can increase GMR sensitivity for transcripts with low copy numbers (Ravi et al., 2018). By using PCR amplification prior to GMR detection in this study, we have successfully performed GMR-based gene expression analysis in samples from a clinically realistic setting of naturally acquired viral respiratory infections. The same information could be gained with NGS, but at a much higher price, turnaround time, and experimental complexity. Moreover, by using magnetic detection compared to traditional optimal detection, GMR sensors have the added advantage of providing a lower limit of detection, higher dynamic range, and lower background noise, which are essential in simultaneously quantifying both higher abundance and lower abundance transcripts in gene expression analysis.

By mining publicly available gene expression datasets, Andres-Terre et al. identified a unique set of biomarkers, the IMS, that is specific to influenza infection and can distinguish influenza from bacterial or other respiratory viral infections. We have developed a rapid, multiplexed assay using the GMR platform to measure the IMS score. In this study, we have validated that the IMS biomarker can classify influenza infection in clinical samples, demonstrating for the first time the use of GMR sensors

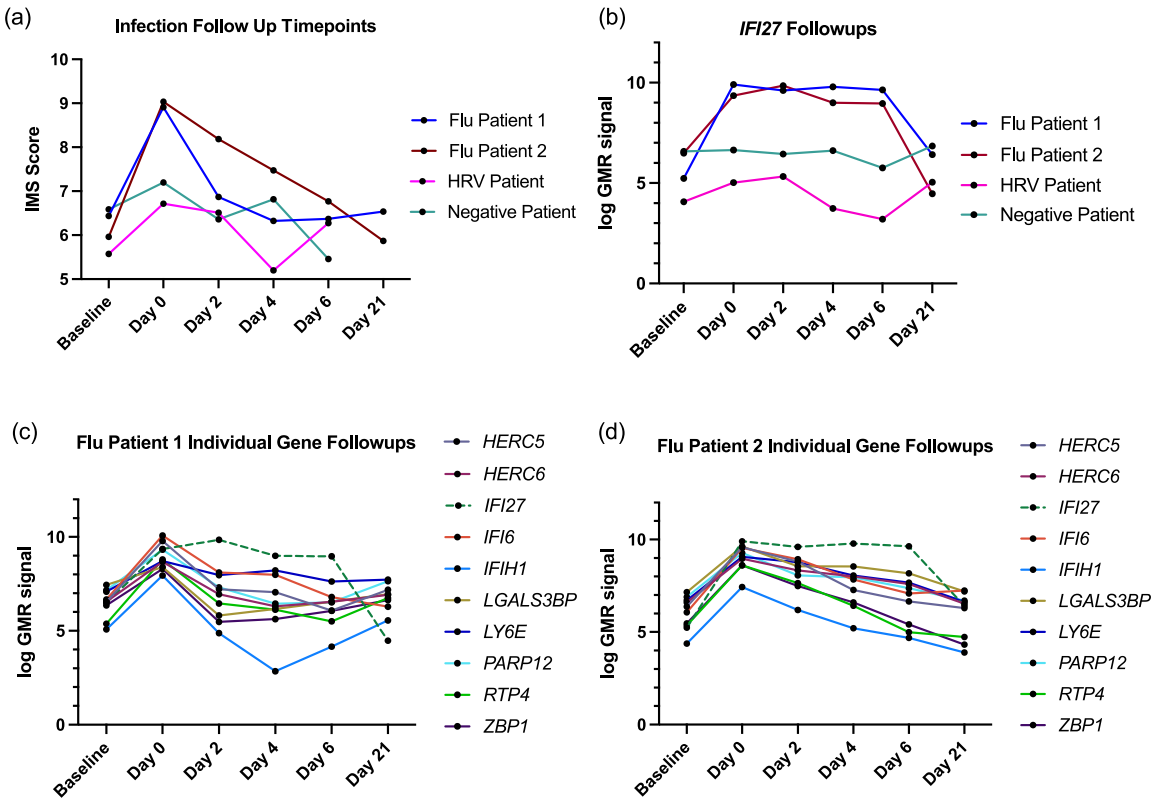

Fig. 6. (a) IMS score (including *IFI27*) over time in subjects with flu-like symptoms (b) *IFI27* expression (log GMR signal) over time in subjects with flu-like symptoms. (c) (d) Expression time course (log GMR signal) of individual genes in the IMS score, plus *IFI27*, in two subjects infected with influenza.

for infectious disease molecular diagnostics. We have shown that the IMS score measured by a GMR biosensor can successfully distinguish IFN-stimulated PBMCs from LPS-stimulated PBMCs and differentiate subjects with influenza from HRV-infected subjects or symptomatic subjects with a negative infection classification. Importantly, while traditional rapid influenza tests and PCR-based tests check for presence of the virus, this assay shifts the paradigm to measure the body's response to the virus. This type of biomarker can be incorporated into future studies in the contexts of disease severity, disease progression, or clinical management (antiviral dosage, for example).

Separately, our results highlight the potential of *IFI27* expression as a biomarker in influenza classification, in accordance with other studies (Zhai et al., 2015; Tang et al., 2017; Kollmus et al., 2018). Due to the inherent biological and experimental correlation of the IMS genes, we have found that only a few IMS genes, along with *IFI27*, are needed for accurate classification in the cohort we have studied. Comparatively, our findings indicate that *IFI27* is a less time-sensitive biomarker than the IMS genes. While *IFI27* expression is high for at least six days after symptom onset, individual IMS gene expression levels (and the corresponding IMS score) wane quickly after the day of symptom onset. This finding is of potential clinical relevance, as most patients outside a research setting usually do not seek medical attention on the first day of symptoms.

More recently, Gupta et al. have shown that *IFI27* alone has high accuracy in diagnosing SARS-CoV-2 infection. While *IFI27* was a top performing single biomarker for influenza diagnosis in the cohort we have analyzed, future studies will greatly benefit from measuring more than one biomarker to obtain accurate influenza classification. This reinforces the diagnostic utility of the LASSO regression score: by combining *IFI27* with select IMS genes (*HERC5, HERC6*, and *IFIH1)*, the accuracy and specificity of influenza diagnosis can be improved for future studies.

It is important to note that in the existing platform, prior to beginning the GMR readout, the sample must go through RNA purification, reverse transcription, and PCR with target gene-specific biotinylated primers. For this diagnostic assay to be implemented as a POC test with a rapid readout of a patient's response to infection, certain parts of the workflow must be integrated and expedited. While not used in this study, we are currently developing a POC PCR/GMR sensor system for DNA detection, in which cDNA, IMS primers, and PCR reaction materials are loaded onto the GMR chip functionalized with ssDNA probes complementary to IMS genes of interest, and on-chip PCR is performed with endpoint GMR detection (Yao et al., 2021). Future studies will involve translating the IMS assay onto the POC PCR/GMR system and observing the real-time hybridization curves of the amplifying IMS genes to the ssDNA probes on the GMR surface.

The strengths of the present study include thorough recruitment and collection of human samples in a study of naturally occurring viral respiratory infections, a novel assay design with portable magnetic biosensors, and robust data analysis with emphasis on machine learning classifiers. This study also has some limitations. First, RNA samples were collected 12 years prior to analysis. While these were banked in a core facility at -80 °C with central temperature monitoring, long-term storage could impact RNA quality. Second, we could only test the IMS signature on a limited number of respiratory illnesses. Whereas testing in other common viral respiratory infections, such as respiratory syncytial virus (RSV), or in bacterial infections, would have been valuable, such samples were not available in abundance for our studies. Finally, there was a limited number of preserved samples with follow-up time points in the longitudinal analysis.

In summary, we have developed a rapid, GMR-based assay for measuring the host response to influenza infection, demonstrating for

the first time the use of GMR biosensors in infectious disease molecular diagnostics. We have also experimentally validated the biomarker set discovered by Andres-Terre et al., demonstrating that a subset of the genes in the signature, with the addition of the *IFI27* gene, improves the accuracy of classification. We have shown the potential of measuring immune system metrics that can be used along with traditional PCR diagnostics to quantify the immune response and monitor disease progression. More broadly, the ease of use and versatility of the GMR platform lends itself to rapidly measuring any biomarker signature. Future studies could involve developing a unique set of biomarkers specific to any disease, such as COVID-19, and translating this assay seamlessly onto the existing platform.

CRediT authorship contribution statement

Neeraja Ravi: Conceptualization, Methodology, Validation, Formal analysis, Investigation, Writing – original draft, Writing – review & editing, Visualization. **Sarah E. Chang:** Investigation, Writing – review & editing. **Luis M. Franco:** Resources, Writing – review & editing. **Sandesh C.S. Nagamani:** Resources, Writing – review & editing. **Purvesh Khatri:** Methodology, Writing – review & editing, Funding acquisition. **Paul J. Utz:** Writing – review & editing, Funding acquisition, Supervision. **Shan X. Wang:** Conceptualization, Writing – review & editing, Funding acquisition, Supervision.

Declaration of competing interest

The authors declare the following financial interests/personal relationships which may be considered as potential competing interests:

S.X.W. has related patents or patent applications assigned to Stanford University and out-licensed for potential commercialization. S.X.W. has stock or stock options in MagArray, Inc., which has licensed relevant patents from Stanford University for commercialization of GMR nanosensor chips.

Acknowledgements:

We would like to acknowledge Paula P. Hernandez and Gladys E. Zapata at the Baylor College of Medicine, who provided immense support in the successful transfer of the samples to Stanford. N.R. acknowledges support from the Stanford Graduate Fellowship and the Advancing Science in America (ARCS) Fellowship. N.R. and S.X.W. were supported in part by the National Institute of Allergy and Infectious Diseases of the National Institutes of Health (NIH) [R01 AI125197], the Autoimmunity Center of Excellence of the NIH [U19 AI110491], and the National Cancer Institute [R01 CA257843] and [U54 CA199075]. S.E.C. and P.J.U. were supported by the NIH grants [R01 AI125197-04] and [R21 AI59578-01]. P.J.U. was also supported in part by the Henry Gustav Floren Trust, as well as the Bill & Melinda Gates Foundation [OPP1113682]. L.M.F. was supported by the Intramural Research Program of the National Institute of Arthritis and Musculoskeletal and Skin Diseases and the National Institute of Allergy and Infectious Diseases, at the U.S. National Institutes of Health. S.C.S.N. was supported in part by the Clinical Translational Core at Baylor College of Medicine, supported by the IDDRC grant [U54 HD083092] from the Eunice Kennedy Shriver National Institute of Child Health and Human Development. The content is solely the responsibility of the authors and does not necessarily represent the official views of the Eunice Kennedy Shriver National Institute of Child Health and Human Development or the National Institutes of Health.

Appendix A. Supplementary data

Supplementary data to this article can be found online at https://doi.org/10.1016/j.bios.2022.114086.

References

Adem, S., Jain, S., Sveiven, M., Zhou, X., O'Donoghue, A.J., Hall, D.A., 2020. Giant magnetoresistive biosensors for real-time quantitative detection of protease activity. Sci. Rep. 10, 7941. https://doi.org/10.1038/s41598-020-62910-2.

Andres-Terre, M., McGuire, H.M., Pouliot, Y., Bongen, E., Sweeney, T.E., Tato, C.M., Khatri, P., 2015. Integrated, multi-cohort analysis identifies conserved transcriptional signatures across multiple respiratory viruses. Immunity 43, 1199–1211. https://doi.org/10.1016/j.immuni.2015.11.003.

Arts, P., van der Raadt, J., van Gestel, S.H.C., Steehouwer, M., Shendure, J., Hoischen, A., Albers, C.A., 2017. Quantification of differential gene expression by multiplexed targeted resequencing of cDNA. Nat. Commun. 8, 15190. https://doi.org/10.1038/ncomms15190.

CDC, 2016. Rapid Influenza Diagnostic Tests. https://www.cdc.gov/flu/professionals/diagnosis/clinician_guidance_ridt.htm.

CDC, 2021a. CDC diagnostic tests for COVID-19. https://www.cdc.gov/coronavirus/2019-ncov/lab/testing.html.

CDC, 2021b. Disease burden of influenza. https://www.cdc.gov/flu/about/burden/index.html.

Choi, J., Gani, A.W., Bechstein, D., Lee, J.R., Utz, P.J., Wang, S.X., 2016. Portable, one-step, and rapid GMR biosensor platform with smartphone interface. Biosens. Bioelectron. 85, 1–7. https://doi.org/10.1016/j.bios.2016.04.046.

Forum of International Respiratory Societies, 2017. The Global Impact of Respiratory Disease, second ed. European Respiratory Society, Sheffield.

Gao, S., Kang, L., Deng, M., Ji, B., Liu, J., Xin, W., Kang, J., Li, P., Gao, J., Wang, J., Yang, H., 2016. A giant magnetoimpedance-based microfluidic system for multiplex immunological assay. Nano Biomed. Eng. 8 (4), 240–245. https://doi.org/10.5101/nbe.v8i4.p240-245.

Gupta, R., et al., 2021. Blood transcriptional biomarkers of acute viral infection for detection of pre symptomatic SARS-CoV-2 infection: a nested, case-control diagnostic accuracy study. Lancet Microb. 2 (Issue 10), e508–e517. https://doi.org/10.1016/S2666-5247(21)00146-4.

Killip, M.J., Fodor, E., Randall, R.E., 2015. Influenza virus activation of the interferon system. Virus Res. 209, 11–22. https://doi.org/10.1016/j.virusres.2015.02.003.

Kollmus, H., Pilzner, C., Leist, S.R., et al., 2018. Of mice and men: the host response to influenza virus infection. Mamm. Genome 29, 446–470. https://doi.org/10.1007/s00335-018-9750-y.

Krishna, V.D., Wu, K., Perez, A.M., Wang, J.P., 2016. Giant magnetoresistance-based biosensor for detection of influenza A virus. Front. Microbiol. 7, 400. https://doi.org/10.3389/fmicb.2016.00400.

Lee, J.-R., Haddon, D.J., Wand, H.E., Price, J.V., Diep, V.K., Hall, D.A., Petri, M., Baechler, E.C., Balboni, I.M., Utz, P.J., Wang, S.X., 2016. Multiplex giant magnetoresistive biosensor microarrays identify interferon-associated autoantibodies in systemic lupus erythematosus. Sci. Rep. 6 https://doi.org/10.1038/srep27623.

Nesvet, J.C., et al., 2021. Giant magnetoresistive nanosensor analysis of circulating tumor DNA epidermal growth factor receptor mutations for diagnosis and therapy response monitoring. Clin. Chem. 67 (3), 534–542. https://doi.org/10.1093/clinchem/hvaa307.

Opal, S.M., 2010. Endotoxins and other sepsis triggers. Contrib. Nephrol. 167, 14–24. https://doi.org/10.1159/000315915.

Osterfeld, S.J., et al., 2008. Multiplex protein assays based on real-time magnetic nanotag sensing. Proc. Natl. Acad. Sci. U.S.A. 105, 20637–20640. https://doi.org/10.1073/pnas.0810822105.

Park, S.-M., et al., 2016. Molecular profiling of single CTCs. Proc. Natl. Acad. Sci. Unit. States Am. 113 (52), E8379–E8386. http://10.1073/pnas.1608461113.

Ravi, N., Rizzi, G., Chang, S.E., Cheung, P., Utz, P.J., Wang, S.X., 2018. Quantification of cDNA on GMR biosensor array towards point-of-care gene expression analysis. Biosens. Bioelectron. 130, 338–343. https://doi.org/10.1016/j.bios.2018.09.050.

Rizzi, G., Lee, J.-R., Dahl, C., Guldberg, P., Dufva, M., Wang, S.X., Hansen, M.F., 2017. Simultaneous profiling of DNA mutation and methylation by melting analysis using magnetoresistive biosensor array. ACS Nano 11, 8864–8870. https://doi.org/10.1021/acsnano.7b03053.

Szklarczyk, D., Gable, A.L., Nastou, K.C., Lyon, D., Kirsch, R., Pyysalo, S., Doncheva, N. T., Legeay, M., Fang, T., Bork, P., Jensen, L.J., von Mering, C., 2021. The STRING database in 2021: customizable protein-protein networks, and functional characterization of user-uploaded gene/measurement sets. Nucleic Acids Res. 49 (D1), D605–D612. https://doi.org/10.1093/nar/gkaa1074.

Tang, B.M., et al., 2017. A novel immune biomarker *IFI27* discriminates between influenza and bacteria in patients with suspected respiratory infection. Eur. Respir. J. 49 (6), 1602098 https://doi.org/10.1183/13993003.02098-2016.

Wang, W., Wang, Y., Tu, L., et al., 2014. Magnetoresistive performance and comparison of supermagnetic nanoparticles on giant magnetoresistive sensor-based detection system. Sci. Rep. 4, 5716. https://doi.org/10.1038/srep05716.

WHO, 2018. Influenza (seasonal). https://www.who.int/news-room/fact-sheets/detail/influenza.

Xu, L., Yu, H., Akhras, M.S., Han, S.-J., Osterfeld, S., White, R.L., Pourmand, N., Wang, S. X., 2008. Giant magnetoresistive biochip for DNA detection and HPV genotyping. Biosens. Bioelectron. 24, 99–103. https://doi.org/10.1016/j.bios.2008.03.030.

Yao, C., Antilla, K., de Olazarra, A.S., Ravi, N., Ng, E., Wang, S.X., 2021. A Method and Device for Automated and Point-Of-Care Nucleic Acid Amplification Test. PCT/US2021/039883.

Zhai, Y., Franco, L.M., Atmar, R.L., Quarles, J.M., Arden, N., Bucasas, K.L., et al., 2015. Host transcriptional response to influenza and other acute respiratory viral infections – a prospective cohort study. PLoS Pathog. 11 (6), e1004869 https://doi.org/10.1371/journal.ppat.1004869.

Zhao, S., Fung-Leung, W.-P., Bittner, A., Ngo, K., Liu, X., 2014. Comparison of RNA-seq and microarray in transcriptome profiling of activated T cells. PLoS One 9 (1), e78644. https://doi.org/10.1371/journal.pone.0078644.

Zhi, X., Liu, Q., Zhang, X., Zhang, Y., Feng, J., Cui, D., 2012. Quick genotyping detection of HBV by giant magnetoresistive biochip combined with PCR and line probe assay. Lab Chip 12, 741–745. https://doi.org/10.1039/C2LC20949G.

Zhi, X., Deng, M., Yang, H., Gao, G., Wang, K., Fu, H., Zhang, Y., Chen, D., Cui, D., 2014. A novel HBV genotypes detecting system combined with microfluidic chip, loop-mediated isothermal amplification and GMR sensors. Biosens. Bioelectron. 54, 372–377. https://doi.org/10.1016/j.bios.2013.11.025.